Acta Oncologica, 2011; 50(Suppl 1): 25–38

informa
healthcare

ORIGINAL ARTICLE

State-of-the-art uroradiologic imaging in the diagnosis of prostate cancer

STIJN W. T. P. J. HEIJMINK[1], JURGEN J. FÜTTERER[1], STEPHEN S. STRUM[2], WIM J. G. OYEN[3], FERDINAND FRAUSCHER[4], J. ALFRED WITJES[5] & JELLE O. BARENTSZ[1]

[1]*Department of Radiology, Radboud University Nijmegen Medical Center, Nijmegen, The Netherlands,* [2]*Medical Oncologist, Ashland, OR 97520, USA,* [3]*Department of Nuclear Medicine, Radboud University Nijmegen Med. Center, Nijmegen, The Netherlands,* [4]*Department of Radiology II, University Hospital Innsbruck, A-6020 Innsbruck, Austria and* [5]*Department of Urology, Radboud University Nijmegen Medical Center, Nijmegen, The Netherlands*

Abstract

In the diagnostic process of prostate cancer, several radiologic imaging modalities significantly contribute to the detection and localization of the disease. These range from transrectal ultrasound (TRUS) and magnetic resonance imaging (MRI) to positron emission tomography (PET). Within this review, after evaluation of the literature, we will discuss the advantages and disadvantages of these imaging modalities in clarifying the patient's clinical status as to whether he has prostate cancer or not and if so, where it is located, so that therapy appropriate to the patient's disease may be administered. TRUS, specifically with the usage of intravenous contrast agents, provides an excellent way of directing biopsy towards suspicious areas within the prostate in the general (screening) population. MRI using functional imaging techniques allows for highly accurate detection and localization, particularly in patients with prior negative ultrasound guided biopsies. A promising new development is the performance of biopsy within the magnetic resonance scanner. Subsequently, a proposal for optimal use of radiologic imaging is presented and compared with the European and American urological guidelines on prostate cancer.

With a total of 217 730 new cases estimated for 2010, prostate cancer (PC) now accounts for 28% of all new male cancers diagnosed in the USA [1]. In their lifetime, one in six men will be clinically diagnosed with having PC, although many more men are found to have histological evidence of PC at autopsy [2–4]. Presently, approximately 1 in 10 men will die of PC [5,6]. The ever-aging population and wider spread use of the prostate-specific antigen (PSA) test [7,8], as well as the tendency to apply lower cut-off levels for this test [9], will further increase the diagnosis of this disease [10].

An elevated PSA level, abnormal changes in PSA level (i.e. PSA dynamics) such as PSA velocity or doubling time, or an abnormal digital rectal examination are biologic indicators signaling an increased risk of PC. With the improvement and wider range of curative therapies, detection and subsequent exact localization of PC have become increasingly important because of their influence on treatment strategy [11,12]. Two such affected treatments are laparoscopic (robotic) radical prostatectomy and intensity-modulated radiation therapy (IMRT [13]). The urologist's inability to palpate the operating field during laparoscopic surgery makes it even more crucial to know where the cancer is located. Similarly, the urologist must know whether the cancer is near a neurovascular bundle since this affects the decision of whether or not to perform nerve-sparing prostatectomy [14]. IMRT also necessitates accurate PC localization. While giving a standard dose to the prostate, a higher (i.e. boost) dose can be given to any dominant intraprostatic lesion(s) as these lesions regularly appear to be the sites of recurrent disease [15]. Furthermore, precision radiation dosimetry will decrease radiation complications, particularly

Correspondence: Stijn W.T.P.J. Heijmink, Department of Radiology, Radboud University Nijmegen Medical Center, PO Box 9101, NL-6500 HB Nijmegen, The Netherlands. E-mail: S.Heijmink@rad.umcn.nl

(Received 12 October 2010; accepted 10 November 2010)

ISSN 0284-186X print/ISSN 1651-226X online © 2011 Informa Healthcare
DOI: 10.3109/0284186X.2010.578369

rectal wall toxicity [16], thereby likely diminishing the development of post-radiation rectal cancer [17].

In order to determine the optimal treatment for the individual patient, it is necessary to evaluate all patient and cancer characteristics. Most often used for this purpose are laboratory values (PSA level and dynamics), the results of digital rectal examination (clinical staging), and histopathological prostatic biopsy findings (Gleason score). However, imaging may play an important role in detecting and localizing areas most reflective of the actual aggressiveness of the cancer. This directly influences the assessment of the patient and may lead to important changes in treatment strategy which can mean the difference between treatment success and failure.

Currently, a spectrum of imaging modalities is available to clinicians for tackling detection- and localization-related problems. To provide optimal and cost efficient patient care, these techniques should be used in the appropriate clinical context to aid clinicians in detecting and localizing PC.

This review 1) presents an overview of the currently available imaging methods to aid in PC detection and localization. 2) Additionally, a scheme is proposed for optimal evidence-based use of imaging in detecting and localizing prostate cancer and a critical comparison is made between this scheme and the most recent guidelines as put forward by the American Urological Association (AUA) and European Association of Urology (EAU).

Literature search

Relevant articles were retrieved using combinations of both Medical Subject Headings (MeSH) and free search terms in the MedLine® (WebSPIRS Version 5.12, Build 20060224, Ovid Technologies) and Pubmed (U.S. National Library of Medicine) online search engines.

MeSH terms included: "Prostate", "Anatomy", "Prostatic Neoplasms", "Neoplasm Staging", "Ultrasonography", "Tomography, X-Ray Computed", "Magnetic Resonance Imaging", "Magnetic Resonance Spectroscopy", "Diffusion Magnetic Resonance Imaging", "Radionuclide Imaging", and "Positron-Emission Tomography".

Free search terms included: "prost*", "cancer", "detect*", "localization", "localisation", "biops*", "stag*", "capsul*", "extracapsular penetration", "extracapsular extension", "seminal vesicle invasion", "transrectal ultraso*", "TRUS", "computed tomography", "CT", "magnetic resonance imaging", "MRI", "ferumoxtran-10", "magnetic resonance spectroscopy", "spectroscopy", "MRS", "bone scan*", "bone scintigraphy", "positron-emission tomography", "PET", and "ProstaScint".

Reference lists of selected articles were further analyzed for relevant articles.

Prostate cancer detection and localization in reference to prostate anatomy and essential prostate cancer characteristics

In order to effectively apply the various imaging modalities, it is important to first understand both the normal prostate anatomy and the distribution and intrinsic characteristics of PC.

Normal anatomy as related to PC localization

On the basis of its embryological origins, the prostate is anatomically divided into three zones that are eccentrically located around the urethra: the innermost transition zone (TZ), the central zone, and the outermost peripheral zone (PZ) [18,19]. In older patients, the former two cannot be distinguished radiologically due to compression of the central zone by benign prostatic hyperplasia (BPH) in the TZ and together they are referred to as the central gland; this as opposed to the outer gland, which comprises the PZ. Furthermore, the prostate is craniocaudally divided into apex (the caudal one-third), mid-gland, and base (the cranial one-third).

Anatomical distribution of PC

Up to 70–80% of PC is located in the PZ [20] and overall analysis of these cancers has shown homogeneous distribution across the entire PZ [21], with over half of the prostates containing two or more distinct cancer foci [22]. Nevertheless, while up to 20–52% of all PC originate in the TZ, only a small (3.6–25%) percentage of these cancers [21,23] occur solely in the TZ as many will have concurrent PZ cancer foci [20,24,25].

Pathological grading of PC aggressiveness

Presently, the most widely used histological scaling system for PC aggressiveness is the Gleason score [26,27], which consists of two numbers: a primary and secondary Gleason grade reflecting the two grades most frequent in the specimen. Each Gleason grade is assigned a value between 1 and 5, the higher numbers indicating a more aggressive cancer. The prognostic value of the Gleason grading system is well-documented [28,29].

Patients clinically at risk for prostate cancer: Radiological imaging to detect and localize primary PC

Transrectal ultrasound (TRUS): Reliable, although not perfect, daily-use modality

Grayscale TRUS. Today, in regular clinical practice, prostate biopsies are performed under TRUS guidance. Even though the traditional ultrasound appearance of PC is a PZ hypoechoic lesion (Figure 1A, B), other conditions such as prostatitis and prostatic intraepithelial neoplasia may also present as hypoechoic lesions [30,31]. It is important to note that over 40% of PC lesions are isoechoic (Figure 1C, D) while only 5% are hyperechoic [32]. Therefore, targeting only hypoechoic areas is not an optimal approach for successful PC detection [33] and various biopsy protocols that sample tissue at standard locations (i.e. systematic biopsy) within the prostate have become the most common biopsy technique [34]. The number of cores taken per session varies across institutions. Recently, however, emphasis has been put on adequate tissue sampling from more laterally located PZ regions [35,36] and on the relative unimportance of biopsying the central gland [37]. Despite the use of extended systematic biopsy protocols, there is still an approximately 20% chance that the Gleason score at prostatectomy will differ from that at biopsy to a clinically relevant degree [38]. Recently, it was observed that biopsies performed with an endfire probe obtained a significantly higher biopsy rate compared with sidefire probes [39]. PC detection rates have varied from 19–40% [40,41] and repeat biopsy sessions are often necessary [42]. Localization sensitivity varied widely between 39–75% (Table I).

Doppler TRUS. Because increased blood flow due to neovascularity is one of the characteristics of PC, this is a means of targeting lesions. In a study of 96 patients with lower urinary tract symptoms and PSA levels over 4 ng/ml [43], the degree of Doppler signal correlated with the microvessel density and Gleason score of a lesion. One study achieved Doppler imaging-based detection rates of 40% [44]. Power Doppler TRUS could improve the localization specificity [45]. However, a drawback of Doppler imaging is the high inter-observer variability [46,47], reflected in the widely spread sensitivity and specificity figures in the literature (27–98% and 46–84%, respectively) (Table I).

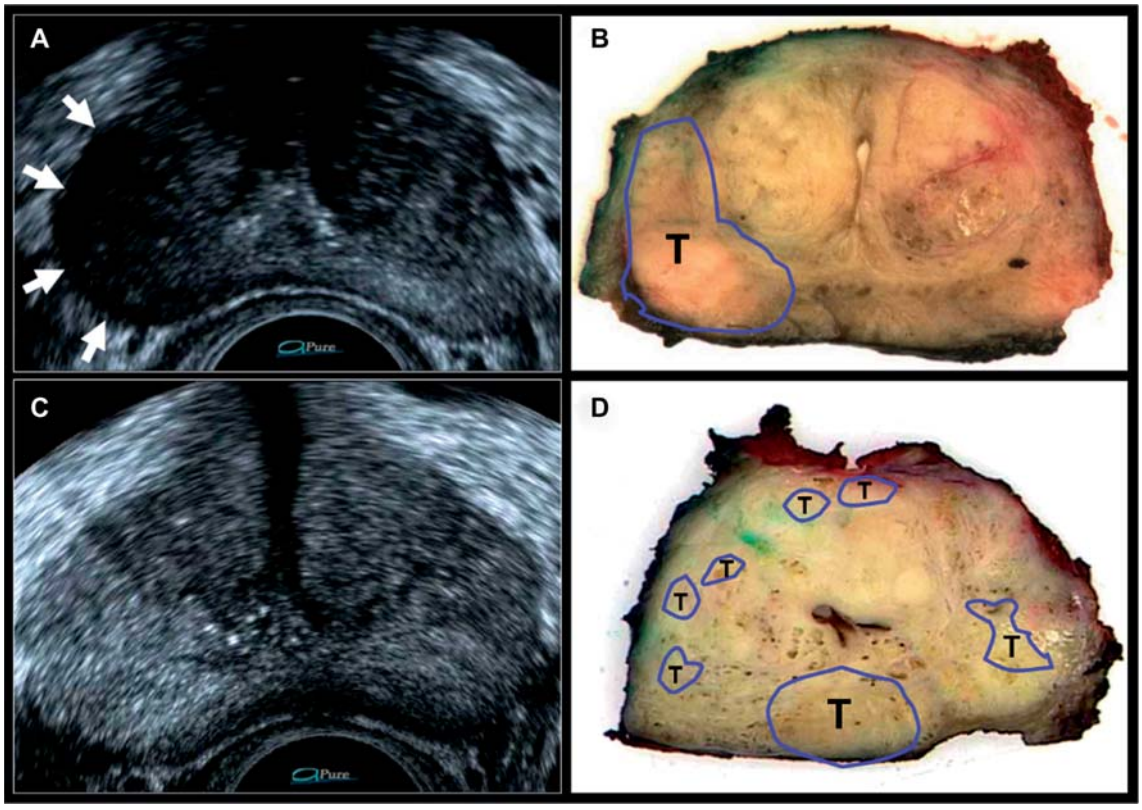

Figure 1. (A) Axial gray-scale transrectal ultrasound image (Aplio™, Toshiba) of the prostate of a 65-year-old man (PSA level 19.02 ng/ml, biopsy Gleason score 6, normal digital rectal examination). A hypoechoic lesion was observed in the right peripheral zone (arrows). (B) Histopathology of the prostatectomy specimen confirmed the presence of a Gleason 3 + 4 adenocarcinoma (T). (C) In another patient (69 years, PSA level 3.59 ng/ml, biopsy Gleason score 7, normal digital rectal examination), the axial gray-scale image did no show any echogenic abnormality while at histopathology (D) a number of cancer foci (T) were reported.

Table I. Overview of studies that examined the diagnostic performance of localizing prostate cancer by imaging modality.

Imaging modality	References	Periods of publication, range	Number of patients, range	Accuracy (%)	Sensitivity (%)	Specificity (%)	PPV (%)	NPV (%)
Transrectal ultrasound								
Gray-scale	[47,75,130]	1998–2000	47–265	52–62	39–75	40–82	45–84	36–72
Doppler	[44,131–135]	1997–2004	136–591	54–83	27–98	46–84	16–84	69–99
Contrast-enhanced	[33,49,50,136,137]	2000–2005	59–380	58–91	48–94	46–88	33–88	55–93
Endorectal MR imaging at 1.5 T								
T2-weighted imaging	[67,73–75,138,139]	1999–2007	24–53	69–82	52–83	46–88	38–80	54–89
Diffusion-weighted imaging	[87]	2010	48	86–89	71–88			
Proton MRSI	[73–75,138,140,141]	1999–2007	24–94	67–87	57–92	57–88	48–83	51–99
Endorectal MR imaging at 3 T								
T2-weighted MR imaging	[102]	2007	46	76–80	53–58	83–86	48–56	85–87
PET scanning								
FDG[11]	[107,110]	1999–2001	24–44	N/A	4–64	100	100	25
C-choline	[115,116]	2005–2006	41–43	71–72	66	81–84	87–88	55–59

PPV, positive predictive value; NPV, negative predictive value; MRSI, magnetic resonance spectroscopic imaging; PET, positron emission tomography; FDG, 18-fluorine-labelled fluorodeoxyglucose, ^{11}C-choline, carbon-11 labeled choline.

Contrast-enhanced TRUS. An innovation is the application of gas-filled microbubble contrast agents, such as Levovist® (Schering, Berlin, Germany) and SonoVue® (Bracco, Milan, Italy) [48]. These microbubbles remain intravascular, thereby enhancing the visibility of the vascular tree in and around the prostate. This improves the ability to detect PC and to thus target areas more representative of the aggressiveness of PC. In experienced hands, it is reported that compared with systematic biopsy, targeting only lesions with pathological enhancement after contrast administration requires less than half the number of biopsy cores to obtain the same diagnostic yield [49–51]. A recent randomized clinical trial comparing systematic biopsy and contrast-enhancement targeted biopsy confirmed these findings [52]. In addition, contrast-enhanced TRUS biopsies on average detected significantly more aggressive cancers compared with systematic biopsy. Therefore, we can speculate that by using this technique the difference in Gleason score between biopsy and prostatectomy specimens would most likely diminish. If the latter is confirmed by future studies, pre-therapeutic risk assessment of patients will increase in accuracy. Disadvantages of using contrast agents are the longer duration and higher degree of invasiveness of the examination; however, the risk of hypersensitivity to the substance is rare and most adverse events are minor and self-resolving [53]. Sensitivities and specificities of PC detection using contrast-enhanced TRUS varied between 48–94% and 46–88%, respectively (Table I). A preliminary study suggests that a 14-day pre-biopsy course of dutasteride, a dual 5α-reductase inhibitor, causes a relative high reduction in blood flow in healthy prostate tissue compared with cancer tissue and could increase the diagnostic yield of contrast-enhanced TRUS targeted biopsy [54].

Sonoelastography. Transrectal sonoelastography is a new non-invasive technique that analyzes the compression characteristics of prostate tissue. A study by König et al. of 404 men undergoing biopsies based on real-time sonoelastography revealed a detection rate of 37.4% [55]. In a comparative study, Pallwein et al. found a significantly higher per core detection rate for sonoelastography-targeted biopsy compared with systematic biopsy. Sonoelastography-targeted biopsy was 2.9 times more likely to detect cancer [56]. A drawback of the latter study was the heterogeneity of the population since more than half of the patients had already undergone one or more negative biopsy sessions. A study comparing real-time sonoelastography with radical prostatectomy reported a localization sensitivity of 88% [57]. While

sonoelastography-based targeted biopsy improves the diagnostic yield it is not yet clear whether it can replace systematic biopsy [58]. Future randomized studies are required to determine the true value of sonoelastography in prostate cancer detection and localization.

Computed Tomography (CT) scanning: Inadequate soft tissue contrast and radiation burden

The literature search resulted in identifying only one recent study on the ability of CT scanning to document histologic PC sites within the prostate gland. This study revealed that contrast-enhanced helical CT scanning was able to detect only 58% of the 102 histologic PC sites documented by TRUS-guided biopsies in 25 patients [59]. In general, CT scanning has inadequate soft tissue contrast resolution to discern the subtle tissue changes due to PC (Figure 2A) and, therefore, should not be used for PC detection and localization. An additional disadvantage of CT is that it involves ionizing radiation.

Endorectal Magnetic Resonance Imaging (MRI) and Magnetic Resonance Spectroscopic Imaging (MRSI): High soft-tissue resolution, radiation-free, but costly and time consuming

T2-weighted imaging. Contrary to CT scanning, MRI has a high soft-tissue contrast resolution. The use of an endorectal coil (ERC) combined with other external coils at 1.5 tesla (T) increases soft-tissue contrast significantly and is now the accepted standard for MRI of the prostate [60]. A drawback is the extra time required for insertion and checking of the position of the disposable ERC, as well as substantial expense.

On MRI, PC typically appears as an area of low signal intensity within the brighter, healthy PZ using a T2-dominated sequence [61–63] (Figure 3A–E). In the central gland, PC is not as clearly discernable because the central gland generally has lower signal intensity than the PZ and is more inhomogeneous due to BPH-induced architectural changes that may mimic PC. A recent study showed that a homogeneous low T2 signal intensity and lenticular shape were significantly associated with presence of central

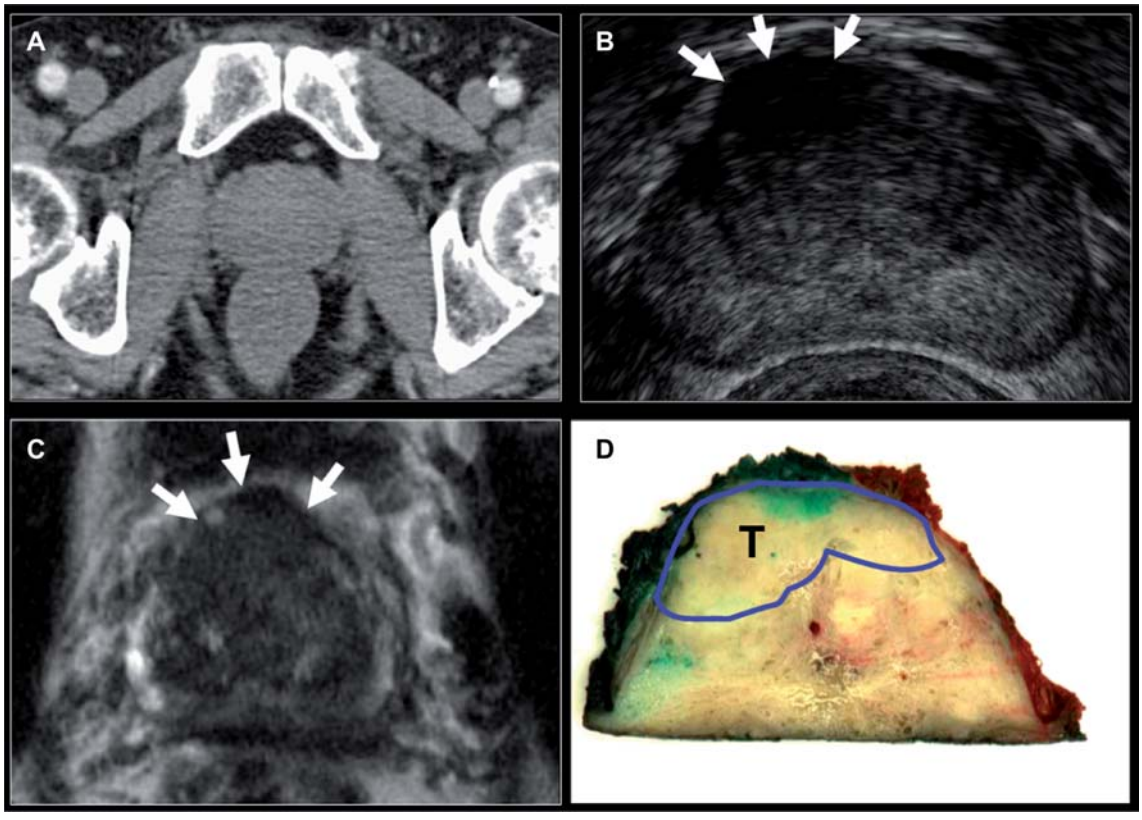

Figure 2. A comparison of the soft-tissue resolution between CT scanning, transrectal ultrasound, and MRI in a 67-year-old man with a PSA level of 38.72 ng/ml, a biopsy Gleason score of 6, and normal digital rectal examination. (A) On the axial CT-scan image the prostate (P) could be discerned. After contrast administration (arrow) no clear enhancement within the prostate was seen. (B) On gray-scale transrectal ultrasound imaging (Viking®, BK Medical) an area of hypoechogenicity (arrows) was visible ventrally. (C) The ventral cancer focus (arrows) was also visible on axial MRI at 3 T with external surface coils. (D) Histopathology confirmed the presence of a ventral cancer focus (Gleason score 7) corresponding to the area of echogenicity on transrectal ultrasound and low signal intensity on MRI.

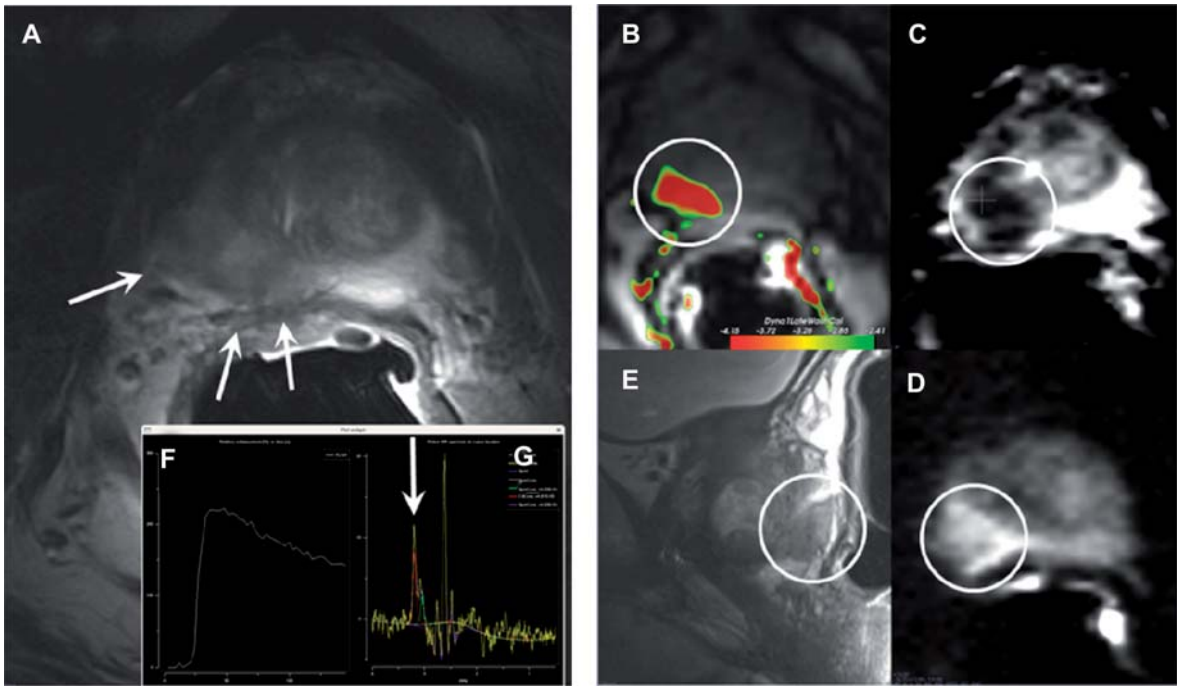

Figure 3. 59-year-old patient with PSA 12, Gleason, eight tumor (circle) right PZ, stage T3a (arrows) at prostatectomy. (A) T2-w axial image, (B) DCE image showing wash-out at the tumor site, (C) ADC-map tumor shows marked restriction, which argues for high Gleason grade, (D) DWI image (b 800) tumor has high signal, (E) sagital T2-weighted image, (F) concentration time curve shows fast wash-in and fast wash-out. G. MR spectrum shows high choline (arrow). This patient scores for all modalities five points (20/20). Scale: 1 no tumor, 5 definitely tumor.

gland PC [64]. It was reported that higher Gleason score cancers had lower signal intensities (relative to muscle) compared with low Gleason score cancers [63]. T2-weighted imaging can be performed in multiple planes or as a three dimension (3D) volume acquisition [65]. Comparing T2-weighted MRI with prostatectomy specimens, MR attained high (52–83%) sensitivities in PC localization, while specificities were somewhat lower (46–88%) (Table I).

A study that directly compared endorectal MRI with digital rectal and TRUS-guided biopsy localization revealed significant incremental value from MRI [66]. In patients subjected to multiple prior negative TRUS-guided biopsies, anatomical MRI by means of T2-dominated acquisition plays an important role. In this patient population, an 83% sensitivity and 50% positive predictive value for MRI have been established [67].

Postbiopsy hemorrhage causes areas of low signal intensity on T2-weighted imaging, thereby making prostate cancer detection more difficult. However, it was shown recently that the amount of hemorrhage was significantly lower in areas of cancer compared with healthy tissue [68].

MRSI. Additionally, MRSI (Figure 3G) can be added to the protocol to provide metabolic information based on the citrate, choline, and creatine levels, and their ratios within the prostate. This is highly informative since the ratio between choline and citrate alters during the transformation from healthy to malignant prostatic cells [69,70] and an increasing choline + creatine/citrate ratio was correlated with higher Gleason scores [71]. Presently, 3D MRSI of the entire prostate can be performed [72], thereby aiding in the diagnosis of central gland PC. The addition of 3D MRSI to MRI has increased localization accuracy, particularly by raising specificity up to 91% [73]. However, a limitation of MRSI is its low spatial resolution. Compared to systematic biopsy, PC localization by means of MRI and MRSI was found to be more sensitive (67% and 76% versus 50%) but less specific (69% and 57% versus 82%) than systematic biopsy [74]. With whole-mount section histopathology as standard of reference, 3D MRSI had a significantly larger area under the receiver operating curve (AUC) of 0.80 in localizing cancer, compared with 0.68 with T2-weighted MRI [75]. Adding the combination of T2-weighted imaging and MRSI to clinical data was shown to have the highest accuracy (AUC 0.85) in predicting the probability of a patient having insignificant prostate cancer [76], significantly higher than that of clinical nomograms. A recent multi-institutional American College of Radiology Imaging Network study raised doubts on the additive value of MRSI over T2-weighted imaging alone [77]. However, potential factors for this result were the selected

prostatectomy population, the small average cancer focus size, and the inclusion of centers without any previous MRSI experience.

Diffusion weighted imaging (DWI). DWI is a novel non invasive technique that measures the fractional anisotropy of water molecules within the prostate which is expressed in apparent diffusion coefficient (ADC) mapping. Thereby, cancer tissue is deemed to result in a more restricted movement of water molecules and thus producing lower ADC values (Figure 3C, D) [78,79]. A recent study in 38 patients, performed at 1.5T with an ERC observed that the mean ADC values of regions of interest placed within prostate cancer tissue was significantly lower than those placed within healthy prostate tissue [80]. In preliminary studies, combining this technique with MRSI [80] or T2-weighted imaging [81] significantly improved the localization accuracy. A recent study in 37 patients revealed a significant increase in sensitivity from 51% for T2-weighted imaging to 71% for combined T2-weighted and DWI reading [82]. In a recent multiparametric analysis, DWI was the best-performing parameter [83]. Preliminary studies at 3T show promising results [84–86]. The b value used appears to affect the PC localization accuracy, as in a preliminary study imaging with a b value of 2000 s/mm^2 was shown to have a significantly higher accuracy compared with 1000 s/mm^2 [87], possibly due to a fall in the signal-to-noise ratio. At biopsy, DWI may aid in differentiating between low-risk and high-risk patients [88].

Dynamic contrast-enhanced MRI [83,89]. To further enhance localization accuracy of MRI, one may use contrast agents. Dynamic contrast-enhanced endorectal MRI, in which the contrast agent concentration is followed in time [90], is able to

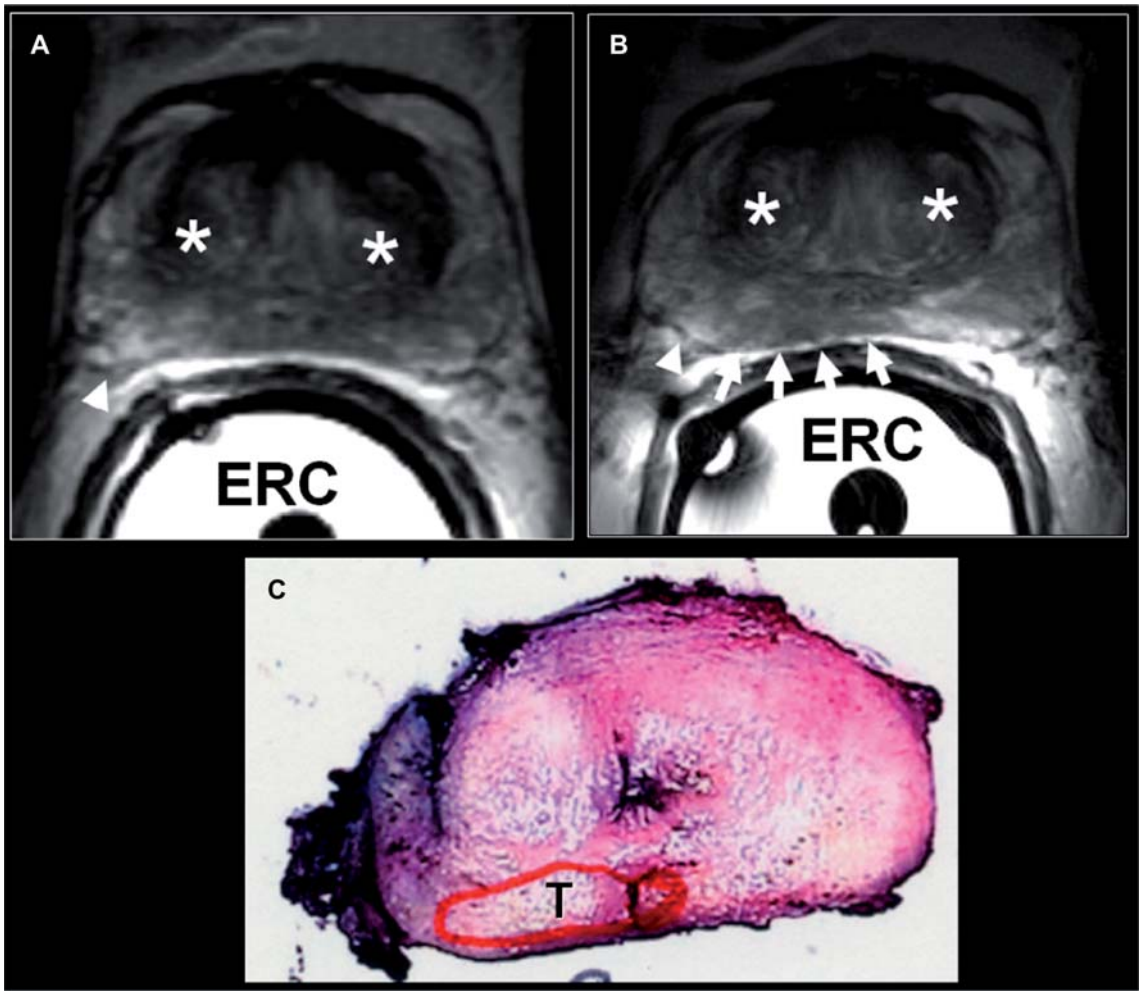

Figure 4. A comparison of the image quality between axial endorectal coil (ERC) MRI at 1.5 T (A) and 3 T (B) in the same patient (age: 58 years, PSA level: 2.7 ng/ml, Gleason biopsy score: 6, normal digital rectal examination). The visibility of the internal architecture of the central gland (*) increased and the capsule (arrowheads) is better delineated at a field strength of 3 T and the tumor (T) as outlined by the histopathology (C) is also better appreciated (arrows).

discriminate between healthy prostatic tissue and PC [91]. Early contrast enhancement and high (relative) peak enhancement are the most accurate predictors of PC of the PZ, while fast washout of contrast agent and high permeability of the blood vessels (Figure 3B, F) are most sensitive for central gland PC [92,93]. A recent study showed that the AUC for localizing PC increased significantly from 0.68 with regular anatomical MRI to 0.91 by applying contrast agent [75]. However, limitations of using contrast agents are the higher costs and possible adverse reactions, of which the most serious, anaphylaxis, is rare [94,95].

Multiparametric imaging. Combining any number of these techniques ('multiparametric imaging') has shown to increase the ability of MRI to detect and localize prostate cancer (Figure 3A–G) [96–98].

High-field imaging. An important future direction is the use of higher magnetic field strengths (e.g. 3T) [99–101] (Figure 4). Compared with body array coil MRI, the higher resolution obtained with ERC MRI at 3T significantly improved PC localization accuracy [102].

Biopsy. Another development is to directly biopsy the prostate by means of MRI [103]. Preliminary results of direct MR-guided transrectal biopsy of suspicious lesions on pre-biopsy MRI in patients with prior negative or inconclusive TRUS-guided biopsy results demonstrated the feasibility of MR prostate biopsy without complications. Nevertheless, disadvantages of the biopsy device are its limited reach, particularly towards the base of the prostate, and procedure duration [104]. In a study of 68 patients with at least two prior negative TRUS biopsy sessions, MR guided biopsy established cancer in 59% [105].

Positron Emission Tomography (PET) Scanning: Metabolic information yet not sufficiently discriminatory from benign disease

FDG. The utility of PET scanning with fluorine-18-labelled deoxyglucose (FDG) in detecting PC is compromised by the relatively low uptake of FDG by prostate cancer cells [106] and significant overlap with marker uptake by BPH. Moreover, reports of FDG uptake correlating with PC aggressiveness have been conflicting, although FDG uptake was substantially higher in metastasized compared to organ-confined primary cancers [107]. A further drawback is that the normal urinary FDG excretion results in high bladder activity which obscures pathological FDG uptake in the prostate. Generally, FDG PET is not recommended for evaluation of the prostate as sensitivities are as low as of 4–64% with a specificity in the order of 50% [108–110].

^{11}C-choline. Another tracer, carbon-11-labelled choline (^{11}C-choline), accumulates in prostatic cells and has the advantage that, unlike FDG, it is not excreted via the urinary tract, and thereby does not influence the visualization of the prostate [111]. Furthermore, the prostate is the only organ in the pelvis to accumulate ^{11}C-choline. The ^{11}C-choline uptake was higher in PC compared with BPH, but the difference was not significant [112]. In a direct comparison between ^{11}C-choline PET and MRSI, a significant linear correlation was observed between the maximum standardized uptake value (SUV) of ^{11}C-choline and the MRSI metabolite ratios. Also, ^{11}C-choline PET was more accurate than MRSI in accurately predicting the laterality (i.e. left- or right-sidedness) of the cancer: 81% (13/16) versus 50% (8/16), respectively [113]. Recently, it was shown that ^{11}C-choline preferentially detected more aggressive prostate cancer foci [114]. Drawbacks are the high costs of ^{11}C-choline and the short half-life of ^{11}C-choline (20 minutes). This latter precludes application of ^{11}C-choline in centers without cyclotrons. Nevertheless, the results of the first two studies combining ^{11}C-choline PET/CT scanning were encouraging, with a sensitivity of 66% and specificity between 81–84% on a sextant basis [115,116]. However, the high rate of false negative findings was a concern. A direct preoperative comparison between 11C-choline PET, FDG PET, and MRI in 43 patients showed that 11C-choline outperformed FDG PET in localizing prostate cancer but that MRI was superior to both [117].

Other radiopharmaceuticals. A preliminary PET/CT study using fluoro-18-choline (^{18}F-choline) demonstrated its feasibility, but reported its inability to distinguish cancer from BPH [118]. In a small population of both primary and recurrent disease, dual-phase ^{18}F-choline showed that areas of malignancy had stably high or increasing uptake while benign areas had decreasing uptake [119]. Thereby, this technique may aid in differentiating malignant from benign prostatic tissue. In a double-tracer study, ^{11}C-acetate PET was more sensitive than FDG, showing consistently increased uptake in PC lesions [120]. A further advantage was that ^{11}C-acetate did not

accumulate in the urine. Again, a considerable uptake overlap was described between normal prostatic tissue, BPH and PC [121].

ProstaScint® scanning: No place in regular clinical practice

ProstaScint® (Cytogen, Princeton, NJ) is an Indium-111 labeled monoclonal mouse antibody specific for prostate-specific membrane antigen. A significant association between the PSA level and detection of ProstaScint® activity in the prostate was reported [122]. A recent study revealed sensitivities between 37–87% and specificities between 0–50%, concluding that the scan could not be used to reliably localize prostate cancer foci within the prostate [123]. In a single study of only seven patients in which the results of ProstaScint® fusion with CT scanning were correlated with systematic biopsy a sensitivity and specificity of 79% and 80%, respectively, were found [124]. In 47 of 51 (92%) preoperative patients at high risk of metastatic disease an increased ProstaScint® activity in the prostate was observed [125].

A drawback is that the antibodies clear slowly from the vasculature and muscle. Blood and bone marrow activity may cause false-positive findings. In regular clinical practice, this modality has no place in primary prostate cancer detection and localization.

Conclusions and discussion

In summary, new developments in ultrasound imaging (Doppler imaging and particularly the application of contrast agents) have proved capable of increasing the PC detection rate with fewer biopsy cores necessary as well as detecting relatively more aggressive cancer foci. This is a substantial improvement for the patient, who will have to undergo fewer biopsies. In addition, treatment guidance is improved since more representative areas are discovered at biopsy and thus the subsequent diagnostic process can be more accurately performed. TRUS remains the primary imaging tool because of its ease-of-use and its role in guiding prostate biopsy. However, TRUS accuracies varied widely among studies, in part due to the inherent high inter-observer variation, particularly in Doppler imaging.

MRI achieves high accuracy rates, particularly when functional information from dynamic

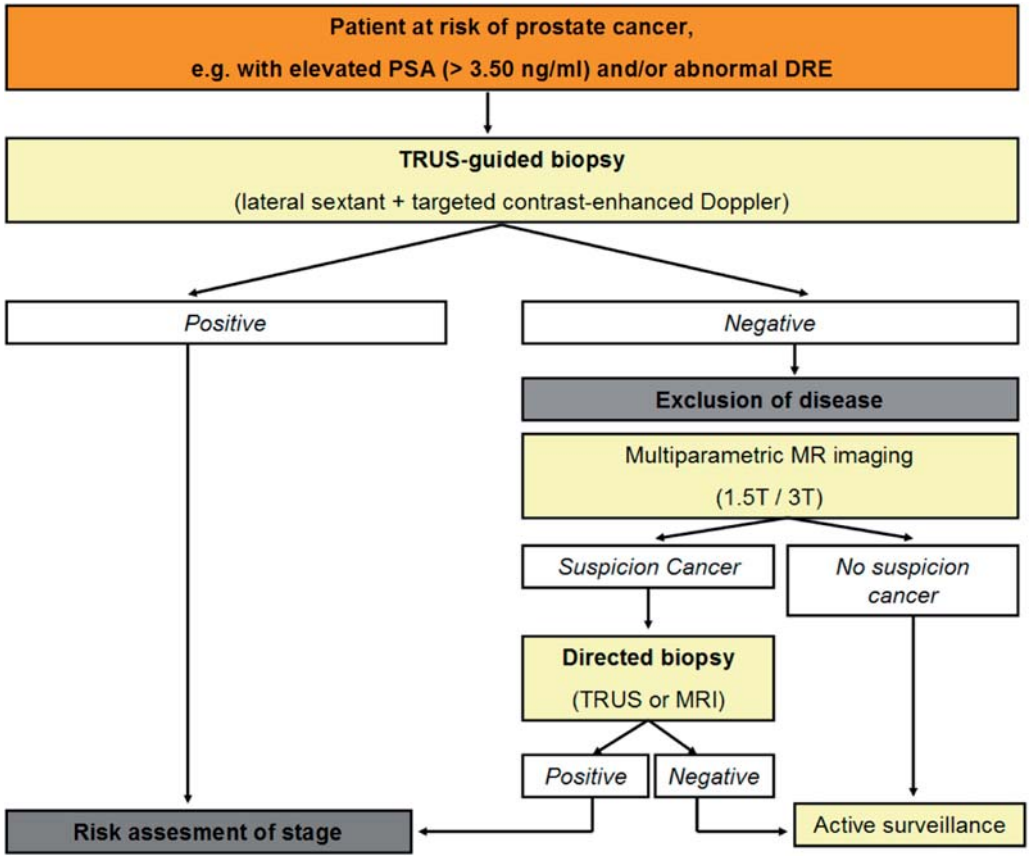

Figure 5. Proposed scheme for optimal use of imaging in patients at risk of prostate having prostate cancer. *Abbreviations*: PSA, prostate-specific antigen; DRE, digital rectal examination; TRUS, transrectal ultrasound; PPA, pelvic phased-array coil.

contrast-enhanced MR and MRSI are added. A multiparametric approach was shown to optimize the diagnostic accuracy. This compensates for the longer examination time and the discomfort of the use of an ERC. Nevertheless, on a cost-effectiveness basis, MRI cannot be performed in all patients at risk of PC [126]. In patients with one or more prior negative TRUS-guided biopsy sessions and continuing suspicion of PC, MRI can provide valuable additional information for PC detection and localization and thereby reduce the future number of biopsies the patient must undergo. Direct MRI guided biopsy is a novel method of performing targeted prostate biopsy.

CT scanning does not play a role in PC detection or localization because of its low soft-tissue resolution and radiation burden. This also applies to PET scanning due to its high costs and invasive nature, as well as the availability of alternative imaging modalities. PET scanning may possibly be used in instances in which TRUS-guided biopsies are negative and absence of evidence of PC on MRI. In addition, combining or fusing PET scanning with, for instance, MRI may be of additional value.

Proposals for optimal usage of imaging

Scheme

Based on the abovementioned, the authors propose the following scheme for patient care in patients at risk for prostate cancer (Figure 5).

Comparison with AUA and EAU guidelines [127–129]

Both associations recognize that the stage migration during the PSA era necessitates more accurate techniques in detecting and localizing prostate cancer. Use of TRUS to guide biopsy is regarded the standard of reference. The EAU's guideline, however, does not mention any contrast-enhanced Doppler imaging based biopsy strategies. This is in contrast to the data presented in our review. Neither CT scanning nor MRI is recommended or mentioned in relation to prostate cancer diagnosis. The latter is in contrast with our proposal in which MRI is used in patients in whom no cancer was found on first TRUS biopsy but with persistently high or rising PSA levels.

Acknowledgements

The authors would like to thank Yvonne L. Hoogeveen for her assistance in preparing the manuscript and Pieter H. M. de Mulder for his guiding recommendations while editing the manuscript.

Declaration of interest: The authors report no conflicts of interest. The authors alone are responsible for the content and writing of the paper.

References

[1] Jemal AJ, Siegel R, Xu J, Ward E. CA Cancer J Clin 2010; 60(5):277–300.
[2] Carter HB, Piantadosi S, Isaacs JT. Clinical evidence for and implications of the multistep development of prostate cancer. J Urol 1990;143:742–6.
[3] Parkin DM, Bray FI, Devesa SS. Cancer burden in the year 2000. The global picture. Eur J Cancer 2001;37(Suppl 8): S4–66.
[4] Konety BR, Bird VY, Deorah S, Dahmoush L. Comparison of the incidence of latent prostate cancer detected at autopsy before and after the prostate specific antigen era. J Urol 2005;174:1785–8.
[5] Crawford ED. Epidemiology of prostate cancer. Urology 2003;62(Suppl 1):3–12.
[6] Stewart SL, King JB, Thompson TD, Friedman C, Wingo PA, et al. Cancer mortality surveillance – United States, 1990–2000. MMWR Surveill Summ 2004;53:1–108.
[7] Catalona WJ, Loeb S, Han M. Viewpoint: Expanding prostate cancer screening. Ann Intern Med 2006;144:441–3.
[8] Hoffman RM. Viewpoint: Limiting prostate cancer screening. Ann Intern Med 2006;144:438–40.
[9] Graif T, Loeb S, Roehl KA, Gashti SN, Griffin C, Yu X, et al. Under diagnosis and over diagnosis of prostate cancer. J Urol 2007;178(1):88–92.
[10] Max W, Rice DP, Sung H, Michel M, Breuer W, Zhang X, et al. The economic burden of prostate cancer, California, 1998. Cancer 2002;94:2906–13.
[11] Mangar SA, Huddart RA, Parker CC, Dearnaley DP, Khoo VS, Horwich A. Technological advances in radiotherapy for the treatment of localised prostate cancer. Eur J Cancer 2005;41:908–21.
[12] Meraney AM, Haese A, Palisaar J, Graefen M, Steuber T, Huland H, et al. Surgical management of prostate cancer: Advances based on a rational approach to the data. Eur J Cancer 2005;41:888–907.
[13] Bucci MK, Bevan A, Roach M, III. Advances in radiation therapy: Conventional to 3D, to IMRT, to 4D, and beyond. CA Cancer J Clin 2005;55:117–34.
[14] Hricak H, Wang L, Wei DC, Coakley FV, Akin O, Reuter VE, et al. The role of preoperative endorectal magnetic resonance imaging in the decision regarding whether to preserve or resect neurovascular bundles during radical retropubic prostatectomy. Cancer 2004;100:2655–63.
[15] Cellini N, Morganti AG, Mattiucci GC, Valentini V, Leone M, Luzi S, et al. Analysis of intraprostatic failures in patients treated with hormonal therapy and radiotherapy: Implications for conformal therapy planning. Int J Radiat Oncol Biol Phys 2002;53:595–9.
[16] Roach M, III. Reducing the toxicity associated with the use of radiotherapy in men with localized prostate cancer. Urol Clin North Am 2004;31:353–66.
[17] Baxter NN, Tepper JE, Durham SB, Rothenberger DA, Virnig BA. Increased risk of rectal cancer after prostate radiation: A population-based study. Gastroenterology 2005;128: 819–24.

[18] McNeal JE. Normal anatomy of the prostate and changes in benign prostatic hypertrophy and carcinoma. Semin Ultrasound CT MR 1988;9:329–34.
[19] Coakley FV, Hricak H. Radiologic anatomy of the prostate gland: A clinical approach. Radiol Clin North Am 2000;38: 15–30.
[20] Chen ME, Johnston DA, Tang K, Babaian RJ, Troncoso P. Detailed mapping of prostate carcinoma foci: Biopsy strategy implications. Cancer 2000;89:1800–9.
[21] McNeal JE, Redwine EA, Freiha FS, Stamey TA. Zonal distribution of prostatic adenocarcinoma. Correlation with histologic pattern and direction of spread. Am J Surg Pathol 1988;12:897–906.
[22] Miller GJ, Cygan JM. Morphology of prostate cancer: The effects of multifocality on histological grade, tumor volume and capsule penetration. J Urol 1994;152(Pt 2):1709–13.
[23] Brossner C, Winterholer A, Roehlich M, Diouhy-Schutz E, Serra V, Sonnleithner M, et al. Distribution of prostate carcinoma foci within the peripheral zone: Analysis of 8,062 prostate biopsy cores. World J Urol 2003;21:163–6.
[24] Horninger W, Reissigl A, Rogatsch H, Volgger H, Studen M, Klocker H, et al. Prostate cancer screening in the Tyrol, Austria: Experience and results. Eur J Cancer 2000;36: 1322–35.
[25] Ohori M, Kattan M, Scardino PT, Wheeler TM. Radical prostatectomy for carcinoma of the prostate. Mod Pathol 2004;17:349–59.
[26] Gleason DF. Histologic grade, clinical stage, and patient age in prostate cancer. NCI Monogr 1988;7:15–8.
[27] Gleason DF. Histologic grading of prostate cancer: A perspective. Hum Pathol 1992;23:273–9.
[28] Egevad L, Granfors T, Karlberg L, Bergh A, Stattin P. Prognostic value of the Gleason score in prostate cancer. BJU Int 2002;89:538–42.
[29] Rasiah KK, Stricker PD, Haynes AM, Delprado W, Turner JJ, Golovsky D, et al. Prognostic significance of Gleason pattern in patients with Gleason score 7 prostate carcinoma. Cancer 2003;98:2560–5.
[30] Lee F, Gray JM, McLeary RD, McHugh TA, Solomon MH, Kumasaka GH, et al. Prostatic evaluation by transrectal sonography: Criteria for diagnosis of early carcinoma. Radiology 1986;158:91–5.
[31] Meirelles LR, Billis A, Cotta AC, Nakamura RT, Caserta NMG, Prando A. Prostatic atrophy: Evidence for a possible role of local ischemia in its pathogenesis. Int Urol Nephrol 2002;34:345–50.
[32] Ellis WJ, Brawer MK. The significance of isoechoic prostatic carcinoma. J Urol 1994;152(Pt 2):2304–7.
[33] Frauscher F, Klauser A, Berger AP, Halpern EJ, Feuchtner G, Koppelstaetter F, et al. The value of ultrasound (US) in the diagnosis of prostate cancer. Radiologie. 2003;43: 455–63.
[34] Hodge KK, McNeal JE, Terris MK, Stamey TA. Random systematic versus directed ultrasound guided transrectal core biopsies of the prostate. J Urol 1989;142:71–4.
[35] Presti JC, Jr. Prostate biopsy: How many cores are enough? Urol Oncol 2003;21:135–40.
[36] Eskicorapci SY, Baydar DE, Akbal C, Sofikerim M, Gunay M, Ekici S, et al. An extended 10-core transrectal ultrasonography guided prostate biopsy protocol improves the detection of prostate cancer. Eur Urol 2004;45:444–8.
[37] Pelzer AE, Bektic J, Berger AP, Halpern EJ, Koppelstätter F, Klauser A, et al. Are transition zone biopsies still necessary to improve prostate cancer detection? Results from the Tyrol screening project. Eur Urol 2005;48(6):916–21.
[38] King CR, McNeal JE, Gill H, Presti JC, Jr. Extended prostate biopsy scheme improves reliability of Gleason grading: Implications for radiotherapy patients. Int J Radiat Oncol Biol Phys 2004;59:386–91.
[39] Ching CB, Moussa AS, Li J, Lane BR, Zippe C, Jones JS, et al. Does transrectal ultrasound probe configuration really matter? End fire versus side fire probe prostate cancer detection rates. J Urol 2009;181:2077–82.
[40] Gore JL, Shariat SF, Miles BJ, Kadmon D, Jiang N, Wheeler TM, et al. Optimal combinations of systematic sextant and laterally directed biopsies for the detection of prostate cancer. J Urol 2001;165:1554–9.
[41] Scherr DS, Eastham J, Ohori M, Scardino PT. Prostate biopsy techniques and indications: When, where, and how? Semin Urol Oncol 2002;20:18–31.
[42] Djavan B, Remzi M, Schulman CC, Marberger M, Zlotta AR, et al. Repeat prostate biopsy: Who, how and when? A review. Eur Urol 2002;42:93–103.
[43] Wilson NM, Masoud AM, Barsoum HB, Refaat MM, Moustafa MI, Kamal TA, et al. Correlation of power Doppler with microvessel density in assessing prostate needle biopsy. Clin Radiol 2004;59:946–50.
[44] Okihara K, Kojima M, Nakanouchi T, Okada K, Miki T. Transrectal power Doppler imaging in the detection of prostate cancer. BJU Int 2000;85:1053–7.
[45] Eisenberg ML, Cowan JE, Carroll PR, Shinohara K. The adjunctive use of power Doppler imaging in the preoperative assessment of prostate cancer. BJU Int 2010;105(9):1237–41.
[46] Rifkin MD, Sudakoff GS, Alexander AA. Prostate: Techniques, results, and potential applications of color Doppler US scanning. Radiology 1993;186:509–13.
[47] Lavoipierre AM, Snow RM, Frydenberg M, Gunter D, Reisner G, Royce PL, et al. Prostatic cancer: Role of color Doppler imaging in transrectal sonography. AJR Am J Roentgenol 1998;171:205–10.
[48] Jakobsen JA, Correas JM. Ultrasound contrast agents and their use in urogenital radiology: Status and prospects. Eur Radiol 2001;11:2082–91.
[49] Frauscher F, Klauser A, Volgger H, Halpern EJ, Pallwein L, Steiner H, et al. Comparison of contrast enhanced color Doppler targeted biopsy with conventional systematic biopsy: Impact on prostate cancer detection. J Urol 2002;167:1648–52.
[50] Pelzer A, Bektic J, Berger AP, Pallwein L, Halpern EJ, Horninger W, et al. Prostate cancer detection in men with prostate specific antigen 4 to 10 ng/ml using a combined approach of contrast enhanced color Doppler targeted and systematic biopsy. J Urol 2005;173:1926–9.
[51] Mitterberger M, Pinggera GM, Horninger W, Bartsch G, Strasser H, Schäfer G, et al. Comparison of contrast enhanced color doppler targeted biopsy to conventional systematic biopsy: Impact on Gleason score. J Urol 2007;178(2): 464–8.
[52] Mitterberger M, Horninger W, Pelzer A, Strasser H, Bartsch G, Moser P, et al. A prospective randomized trial comparing contrast-enhanced targeted versus systematic ultrasound guided biopsies: Impact on prostate cancer detection. Prostate 2007;67:1537–42.
[53] Jakobsen JA, Oyen R, Thomsen HS, Morcos SK. Safety of ultrasound contrast agents. Eur Radiol 2005;15:941–5.
[54] Mitterberger M, Pinggera G, Horninger W, Hannes Strasser, Halpern E, Pallwein L, et al. Dutasteride prior to contrast-enhanced colour Doppler ultrasound prostate biopsy increases prostate cancer detection. Eur Urol 2008;53: 112–7.
[55] Konig K, Scheipers U, Pesavento A, Lorentz A, Ermert H, Senge T. Initial experiences with real-time elastography guided biopsies of the prostate. J Urol 2005;174:115–7.

[56] Pallwein L, Mitterberger M, Struve P, Horninger W, Aigner F, Bartsch B, et al. Comparison of sonoelastography guided biopsy with systematic biopsy: Impact on prostate cancer detection. Eur Radiol 2007;17(9):2278–85.
[57] Frauscher F, Klauser A, Koppelstaetter F, Berger AP, Horninger W, Bartsch G, et al. Real-time elastography for prostate cancer detection: Preliminary experience. Eur Radiol 2004; 14(S2):150.
[58] Nelson ED, Slotoroff CB, Gomella LG, Halpern EJ. Targeted biopsy of the prostate: The impact of color Doppler imaging and elastography on prostate cancer detection and Gleason score. Urology 2007;70:1136–40.
[59] Prando A, Wallace S. Helical CT of prostate cancer: Early clinical experience. AJR Am J Roentgenol 2000;175: 343–6.
[60] Tempany CM, Zhou X, Zerhouni EA, Rifkin MD, Quint LE, Piccoli CW, et al. Staging of prostate cancer: Results of Radiology Diagnostic Oncology Group project comparison of three MR imaging techniques. Radiology 1994;192:47–54.
[61] Cruz M, Tsuda K, Narumi Y, Kuroiwa Y, Nose T, Kojima Y, et al. Characterization of low-intensity lesions in the peripheral zone of prostate on pre-biopsy endorectal coil MR imaging. Eur Radiol 2002;12:357–65.
[62] Claus FG, Hricak H, Hattery RR. Pretreatment evaluation of prostate cancer: Role of MR imaging and 1H MR spectroscopy. Radiographics 2004;24(Suppl 1):S167–80.
[63] Wang L, Mazaheri Y, Zhang J, Ishill NM, Kuroiwa K, Hricak H. Assessment of biologic aggressiveness of prostate cancer: Correlation of MR signal intensity with Gleason grade after radical prostatectomy. Radiology 2008;246: 168–76.
[64] Akin O, Sala E, Moskowitz CS, Kuroiwa K, Ishill NM, Pucar D, et al. Transition zone prostate cancers: Features, detection, localization, and staging at endorectal MR imaging. Radiology 2006;239:784–92.
[65] Rosenkrantz AB, Neil J, Kong X, Melamed J, Babb JS, Taneja SS, et al. Prostate cancer: Comparison of 3D T2-weighted with conventional 2D T2-weighted imaging for image quality and tumor detection. AJR Am J Roentgenol 2010;194: 446–52.
[66] Mullerad M, Hricak H, Kuroiwa K, Pucar D, Chen H, Kattan MW, et al. Comparison of endorectal magnetic resonance imaging, guided prostate biopsy and digital rectal examination in the preoperative anatomical localization of prostate cancer. J Urol 2005;174:2158–63.
[67] Beyersdorff D, Taupitz M, Winkelmann B, Fischer T, Lenk S, Loening SA, et al. Patients with a history of elevated prostate-specific antigen levels and negative transrectal US-guided quadrant or sextant biopsy results: Value of MR imaging. Radiology 2002;224:701–6.
[68] Tamada T, Sone T, Jo Y, Yamamoto A, Yamashita T, Egashira N, et al. Prostate cancer: Relationships between postbiopsy hemorrhage and tumor detectability at MR diagnosis. Radiology 2008;248:531–9.
[69] Kurhanewicz J, Vigneron DB, Hricak H, Narayan P, Carroll P, Nelson SJ. Three-dimensional H-1 MR spectroscopic imaging of the in situ human prostate with high [0.24-0.7 cm^3] spatial resolution. Radiology 1996;198:795–805.
[70] Coakley FV, Qayyum A, Kurhanewicz J. Magnetic resonance imaging and spectroscopic imaging of prostate cancer. J Urol 2003;170(Pt 2):S69–75.
[71] Zakian KL, Sircar K, Hricak H, Chen H, Shukla-Dave A, Eberhardt S, et al. Correlation of proton MR spectroscopic imaging with Gleason score based on step-section pathologic analysis after radical prostatectomy. Radiology 2005;234: 804–14.
[72] Scheenen TW, Klomp DW, Roll SA, Fütterer JJ, Barentsz JO, Heerschap A. Fast acquisition-weighted three-dimensional proton MR spectroscopic imaging of the human prostate. Magn Reson Med 2004;52:80–8.
[73] Scheidler J, Hricak H, Vigneron DB, Kyle K, Yu KK , Sokolov DL, et al. Prostate cancer: Localization with three-dimensional proton MR spectroscopic imaging – clinicopathologic study. Radiology 1999;213:473–80.
[74] Wefer AE, Hricak H, Vigneron DB, Coakley FV, Lu Y, Wefer J, et al. Sextant localization of prostate cancer: Comparison of sextant biopsy, magnetic resonance imaging and magnetic resonance spectroscopic imaging with step section histology. J Urol 2000;164:400–4.
[75] Fütterer JJ, Heijmink SWTPJ, Scheenen TWJ, Veltman J, Huisman HJ, Vos P, et al. Prostate cancer localization with dynamic contrast-enhanced MR imaging and proton MR spectroscopic imaging. Radiology 2006;241:449–58.
[76] Shukla-Dave A, Hricak H, Kattan MW, Pucar D, Kuroiwa K, Chen H, et al. The utility of magnetic resonance imaging and spectroscopy for predicting insignificant prostate cancer: An initial analysis. BJU Int 2007;99:786–93.
[77] Weinreb JC, Blume JD, Coakley FV, Wheeler T, Cormack JB, Sotto CK, et al. Prostate cancer: Sextant localization at MR imaging and MR spectroscopic imaging before prostatectomy – results of ACRIN prospective multi-institutional clinicopathologic study. Radiology 2009;251:122–33.
[78] Sato C, Naganawa S, Nakamura T, Kumada H, Miura S, Takizawa O, et al. Differentiation of noncancerous tissue and cancer lesions by apparent diffusion coefficient values in transition and peripheral zones of the prostate. J Magn Reson Imaging 2005;21:258–62.
[79] Zelhof B, Pickles M, Liney G, Peter Gibbs P, Rodrigues G, Kraus S, et al. Correlation of diffusion-weighted magnetic resonance data with cellularity in prostate cancer. BJU Int 2009;103:883–8.
[80] Mazaheri Y, Shukla-Dave A, Hricak H, Fine SW, Zhang, J, Inurrigarro G, et al. Prostate cancer: Identification with combined diffusion-weighted MR imaging and 3D 1H MR spectroscopic imaging – correlation with pathologic findings. Radiology 2008;246:480–8.
[81] Haider MA, Van Der Kwast TH, Tanguay J, Evans AJ, Hashmi A, Lockwood G, et al. Combined T2-weighted and diffusion-weighted MRI for localization of prostate cancer. AJR Am J Roentgenol 2007;189:323–8.
[82] Yoshimitsu K, Kiyoshima K, Irie H, Tajima T, Asayama Y, Hirakawa M, et al. Usefulness of apparent diffusion coefficient map in diagnosing prostate carcinoma: Correlation with stepwise histopathology. J Magn Reson Imaging 2008; 27:132–9.
[83] Langer DL, Van Der Kwast TH, Evans AJ, Trachtenberg J, Wilson BC, Haider A. Prostate cancer detection with multi-parametric MRI: Logistic regression analysis of quantitative T2, diffusion-weighted imaging, and dynamic contrast-enhanced MRI. J Magn Reson Imaging 2009;30:327–34.
[84] Gibbs P, Pickles MD, Turnbull LW. Diffusion imaging of the prostate at 3.0 tesla. Invest Radiol 2006;41:185–8.
[85] Pickles MD, Gibbs P, Sreenivas M, Turnbull LW. Diffusion-weighted imaging of normal and malignant prostate tissue at 3.0T. J Magn Reson Imaging 2006;23:130–4.
[86] Miao H, Fukatsu H, Ishigaki T. Prostate cancer detection with 3-T MRI: Comparison of diffusion-weighted and T2-weighted imaging. Eur J Radiol 2007;61:297–302.
[87] Kim CK, Park BK, Kim B. High-b-Value diffusion-weighted imaging at 3 T to detect prostate cancer: Comparisons between b values of 1,000 and 2,000 s/mm^2. AJR Am J Roentgenol 2010;194:W33–7.

[88] Woodfield CA, Tung GA, Grand DJ, Pezzullo JA, Machan JT, Renzulli JF, et al. Diffusion-weighted MRI of peripheral zone prostate cancer: Comparison of tumor apparent diffusion coefficient with Gleason score and percentage of tumor on core biopsy. AJR Am J Roentgenol 2010;194:W316–22.

[89] Langer DL, Van Der Kwast TH, Evans AJ, Plotkin A, Trachtenberg J, Wilson BC, et al. Prostate tissue composition and MR measurements: Investigating the relationships between ADC, T2, K[trans], v[e], and corresponding histologic features. Radiology 2010;255:485–94.

[90] Barentsz JO, Engelbrecht M, Jager GJ, de LaRosette J, van Der Sanden BP, Huisman HJ, et al. Fast dynamic gadolinium-enhanced MR imaging of urinary bladder and prostate cancer. J Magn Reson Imaging 1999;10:295–304.

[91] Padhani AR, Gapinski CJ, Macvicar DA, Parker GJ, Suckling J, Revell PB, et al. Dynamic contrast enhanced MRI of prostate cancer: Correlation with morphology and tumour stage, histological grade and PSA. Clin Radiol 2000;55:99–109.

[92] Engelbrecht MR, Huisman HJ, Laheij RJ, Jager GJ, van Leenders GJLH, Hulsbergen-Van De Kaa CA, et al. Discrimination of prostate cancer from normal peripheral zone and central gland tissue by using dynamic contrast-enhanced MR imaging. Radiology 2003;229:248–54.

[93] Van Dorsten FA, Van Der Graaf M, Engelbrecht MR, van Leenders GJ, Verhofstad A, Rijpkema M, et al. Combined quantitative dynamic contrast-enhanced MR imaging and [1]H MR spectroscopic imaging of human prostate cancer. J Magn Reson Imaging 2004;20:279–87.

[94] Runge VM. Safety of approved MR contrast media for intravenous injection. J Magn Reson Imaging 2000;12:205–13.

[95] Lin SP, Brown JJ. MR contrast agents: Physical and pharmacologic basics. J Magn Reson Imaging 2007;25:884–99.

[96] Kitajima K, Kaji Y, Fukabori Y, Yoshida K, Suganuma N, Sugimura K. Prostate cancer detection with 3 T MRI: Comparison of diffusion-weighted imaging and dynamic contrast-enhanced MRI in combination with T2-weighted imaging. J Magn Reson Imaging 2010;31:625–31.

[97] Sciarra A, Panebianco V, Ciccariello M, Salciccia S, Cattarino S, Lisi D, et al. Value of magnetic resonance spectroscopy imaging and dynamic contrast-enhanced imaging for detecting prostate cancer foci in men with prior negative biopsy. Clin Cancer Res 2010;16:1875–83.

[98] Turkbey B, Pinto PA, Mani H, Bernardo M, Pang Y, McKinney YL, et al. Prostate cancer: Value of multiparametric MR imaging at 3 T for detection–histopathologic correlation. Radiology 2010;255:89–99.

[99] Futterer JJ, Scheenen TW, Huisman HJ, Klomp DW J, van Dorsten, FA, Hulsbergen-van de Kaa, CA, et al. Initial experience of 3 Tesla endorectal coil magnetic resonance imaging and 1H-spectroscopic imaging of the prostate. Invest Radiol 2004;39:671–80.

[100] Beyersdorff D, Taymoorian K, Knosel T, Schnorr D, Felix R, Hamm B, et al. MRI of prostate cancer at 1.5 and 3.0 T: Comparison of image quality in tumor detection and staging. AJR Am J Roentgenol 2005;185:1214–20.

[101] Scheenen TW, Heijmink SW, Roell SA, Hulsbergen-Van de Kaa CA, Knipscheer BC, Alfred Witjes JA, et al. Three-dimensional proton MR spectroscopy of human prostate at 3 T without endorectal coil: Feasibility. Radiology 2007;245:507–16.

[102] Heijmink SWTPJ, Futterer JJ, Hambrock T, Takahashi S, Scheenen TWJ, Huisman HJ, et al. Prostate cancer: Body-array versus endorectal coil MR imaging at 3 T – Comparison of image quality, localization, and staging performance. Radiology 2007;244:184–95.

[103] Yakar D, Hambrock T, Hoeks C, Barentsz JO, Fütterer, JJ. Magnetic resonance-guided biopsy of the prostate: Feasibility, technique, and clinical applications. Top Magn Reson Imaging 2008;19:291–5.

[104] Beyersdorff D, Winkel A, Hamm B, Severin Lenk S, Loening SA, Taupitz M. MR imaging-guided prostate biopsy with a closed MR unit at 1.5 T: Initial results. Radiology 2005;234:576–81.

[105] Hambrock T, Somford DM, Hoeks C, Bouwense SA, Huisman H, Yakar D, et al. Magnetic resonance imaging guided prostate biopsy in men with repeat negative biopsies and increased prostate specific antigen. J Urol 2010;183:520–7.

[106] Shreve PD, Grossman HB, Gross MD, Wahl RL. Metastatic prostate cancer: Initial findings of PET with 2-deoxy-2-[F-18]fluoro-D-glucose. Radiology 1996;199:751–6.

[107] Oyama N, Akino H, Suzuki Y, Kanamaru H, Sadato N, Yonekura Y, et al. The increased accumulation of [18F] fluorodeoxyglucose in untreated prostate cancer. Jpn J Clin Oncol 1999;29:623–9.

[108] Effert PJ, Bares R, Handt S, Wolff JM, Bull U, Jakse G. Metabolic imaging of untreated prostate cancer by positron emission tomography with 18fluorine-labeled deoxyglucose. J Urol 1996;155:994–8.

[109] Haseman MK, Reed NL, Rosenthal SA. Monoclonal antibody imaging of occult prostate cancer in patients with elevated prostate-specific antigen. Positron emission tomography and biopsy correlation. Clin Nucl Med 1996;21:704–13.

[110] Liu IJ, Zafar MB, Lai YH, Segall GM, Terris MK. Fluorodeoxyglucose positron emission tomography studies in diagnosis and staging of clinically organ-confined prostate cancer. Urology 2001;57:108–11.

[111] Hara T, Kosaka N, Kishi H. PET imaging of prostate cancer using carbon-11-choline. J Nucl Med 1998;39:990–5.

[112] Sutinen E, Nurmi M, Roivainen A, Varpula M, Tolvanen T, Lehikoinen P, et al. Kinetics of [[11]C]choline uptake in prostate cancer: A PET study [correction for stydy]. Eur J Nucl Med Mol Imaging 2004;31:317–24.

[113] Yamaguchi T, Lee J, Uemura H, Sasaki T, Takahashi N, Oka T, et al. Prostate cancer: A comparative study of [11]C-choline PET and MR imaging combined with proton MR spectroscopy. Eur J Nucl Med Mol Imaging 2005;32:742–8.

[114] Piert M, Park H, Khan A, Siddiqui J, Hussain H, Chenevert T, et al. Detection of aggressive primary prostate cancer with 11C-choline PET/CT using multimodality fusion techniques. J Nucl Med 2009;50:1585–93.

[115] Farsad M, Schiavina R, Castellucci P, Nanni C, Barbara Corti B, Martorana G, et al. Detection and localization of prostate cancer: Correlation of [11]C-choline PET/CT with histopathologic step-section analysis. J Nucl Med 2005;46:1642–9.

[116] Martorana G, Schiavina R, Corti B, Farsad M, Salizzoni E, Brunocilla E, et al. 11C-Choline positron emission tomography/computerized tomography for tumor localization of primary prostate cancer in comparison with 12-core biopsy. J Urol 2006;176:954–60.

[117] Watanabe H, Kanematsu M, Kondo H, Kako N, Yamamoto N, Yamada T, et al. Preoperative detection of prostate cancer: A comparison with 11C-choline PET, 18F-fluorodeoxyglucose PET and MR imaging. J Magn Reson Imaging 2010;31:1151–6.

[118] Schmid DT, John H, Zweifel R, Cservenyak T, Westera G, Goerres GW, et al. Fluorocholine PET/CT in patients with

prostate cancer: Initial experience. Radiology 2005; 235:623–8.

[119] Sandblom G, Sörensen J, Lundin N, Häggman M, Malmström PU. Positron emission tomography with c11-acetate for tumor detection and localization in patients with prostate-specific antigen relapse after radical prostatectomy. Urology 2006;67:996–1000.

[120] Oyama N, Akino H, Kanamaru H, Suzuki Y, Muramoto S, Yonekura Y, et al. 11C-acetate PET imaging of prostate cancer. J Nucl Med 2002;43:181–6.

[121] Kato T, Tsukamoto E, Kuge Y, Takei T, Shiga T, Shinohara N, et al. Accumulation of [11C]acetate in normal prostate and benign prostatic hyperplasia: Comparison with prostate cancer. Eur J Nucl Med Mol Imaging 2002;29:1492–5.

[122] Sodee DB, Malguria N, Faulhaber P, Resnick MI , Albert J, Bakale G, et al. Multicenter ProstaScint imaging findings in 2154 patients with prostate cancer. The ProstaScint Imaging Centers. Urology 2000;56:988–93.

[123] Mouraviev V, Madden JF, Broadwater G, Mayes JM, Burchette JL Schneider F, et al. Use of 111in-capromab pendetide immunoscintigraphy to image localized prostate cancer foci within the prostate gland. J Urol 2009;182: 938–47.

[124] Ellis RJ, Kim EY, Conant R, Sodee DB, Spirnak JP, Dinchman KH, et al. Radioimmunoguided imaging of prostate cancer foci with histopathological correlation. Int J Radiat Oncol Biol Phys 2001;49:1281–6.

[125] Burgers JK, Hinkle GH, Haseman MK. Monoclonal antibody imaging of recurrent and metastatic prostate cancer. Semin Urol 1995;13:103–12.

[126] Jager GJ, Severens JL, Thornbury JR, de la Rosette JJMCH, Ruijs SHJ, Barentsz JO. Prostate cancer staging: Should MR imaging be used? – A decision analytic approach. Radiology 2000;215:445–51.

[127] Report on the management of clinically localized prostate cancer. Available from: http://www.auanet.org/guidelines/proscan07.cfm. 2007.

[128] Heidenreich A, Aus G, Abbou CC, Bolla M, Joniau S, Matveev V, Schmid HP, et al. Guidelines on prostate cancer 2007. Available from: http://www.uroweb.org/fileadmin/user_upload/Guidelines/Prostate%20Cancer.pdf. 2007.

[129] Thompson I, Thrasher JB, Aus G, Burnett AL, Canby-Hagino ED, Cookson MS, et al. Guideline for the management of clinically localized prostate cancer: 2007 update. J Urol 2007;177:2106–31.

[130] Salomon L, Colombel M, Patard JJ, Lefrère-Belda MA, Bellot J, Chopin D, et al. Value of ultrasound-guided systematic sextant biopsies in prostate tumor mapping. Eur Urol 1999;35:289–93.

[131] Cornud F, Belin X, Piron D, Chrétien Y, Flam T, Casanova JM, et al. Color Doppler-guided prostate biopsies in 591 patients with an elevated serum PSA level: Impact on Gleason score for nonpalpable lesions. Urology 1997;49:709–15.

[132] Halpern EJ, Strup SE. Using gray-scale and color and power Doppler sonography to detect prostatic cancer. AJR Am J Roentgenol 2000;174:623–7.

[133] Kuligowska E, Barish MA, Fenlon HM, Blake M. Predictors of prostate carcinoma: Accuracy of gray-scale and color Doppler US and serum markers. Radiology 2001; 220:757–64.

[134] Sauvain JL, Palascak P, Bourscheid D, Chabi C, Atassi A, Bremon JM, et al. Value of power doppler and 3D vascular sonography as a method for diagnosis and staging of prostate cancer. Eur Urol 2003;44:21–30.

[135] Remzi M, Dobrovits M, Reissigl A, Ravery V, Waldert M, Wiunig C, et al. Can Power Doppler enhanced transrectal ultrasound guided biopsy improve prostate cancer detection on first and repeat prostate biopsy? Eur Urol 2004; 46:451–6.

[136] Unal D, Sedelaar JP, Aarnink RG, van Leenders GJ, Wijkstra H, Debruyne FM, et al. Three-dimensional contrast-enhanced power Doppler ultrasonography and conventional examination methods: The value of diagnostic predictors of prostate cancer. BJU Int 2000;86:58–64.

[137] Halpern EJ, Rosenberg M, Gomella LG. Prostate cancer: Contrast-enhanced us for detection. Radiology 2001; 219:219–25.

[138] Yuen JS, Thng CH, Tan PH, Khin LW, Phee SJ, Xiao D, et al. Endorectal magnetic resonance imaging and spectroscopy for the detection of tumor foci in men with prior negative transrectal ultrasound prostate biopsy. J Urol 2004;171:1482–6.

[139] Graser A, Heuck A, Sommer B, Massmann J , Scheidler J, Maximillian Reiser M, et al. Per-sextant localization and staging of prostate cancer: Correlation of imaging findings with whole-mount step section histopathology. AJR Am J Roentgenol 2007;188:84–90.

[140] Zakian KL, Sircar K, Hricak H, Chen H, Shukla-Dave A, Eberhardt S, et al. Correlation of proton MR spectroscopic imaging with gleason score based on step-section pathologic analysis after radical prostatectomy. Radiology 2005; 234:804–14.

[141] Fütterer JJ, Scheenen TWJ, Heijmink SWTPJ, Huisman HJ, Hulsbergen-van de Kaa CA, Witjes JA, et al. Standardized threshold approach using three-dimensional proton magnetic resonance spectroscopic imaging in prostate cancer localization of the entire prostate. Invest Radiol 2007; 42:116–22.